



**HAL**  
open science

# Bidirectional DC-DC Converter Using Modular Marx Power Switches and Series/Parallel Inductor for High-Voltage Applications

Ricardo Luís, J. A. Silva, José C. Quadrado, Sónia Ferreira Pinto, Duarte De Mesquita E Sousa

► **To cite this version:**

Ricardo Luís, J. A. Silva, José C. Quadrado, Sónia Ferreira Pinto, Duarte De Mesquita E Sousa. Bidirectional DC-DC Converter Using Modular Marx Power Switches and Series/Parallel Inductor for High-Voltage Applications. 5th Doctoral Conference on Computing, Electrical and Industrial Systems (DoCEIS), Apr 2014, Costa de Caparica, Portugal. pp.478-485, 10.1007/978-3-642-54734-8\_53 . hal-01274812

**HAL Id: hal-01274812**

**<https://inria.hal.science/hal-01274812v1>**

Submitted on 16 Feb 2016

**HAL** is a multi-disciplinary open access archive for the deposit and dissemination of scientific research documents, whether they are published or not. The documents may come from teaching and research institutions in France or abroad, or from public or private research centers.

L'archive ouverte pluridisciplinaire **HAL**, est destinée au dépôt et à la diffusion de documents scientifiques de niveau recherche, publiés ou non, émanant des établissements d'enseignement et de recherche français ou étrangers, des laboratoires publics ou privés.



Distributed under a Creative Commons Attribution 4.0 International License

# Bidirectional DC-DC Converter Using Modular Marx Power Switches and Series/Parallel Inductor for High-Voltage Applications

Ricardo Luís<sup>1</sup>, J. Fernando Silva<sup>2</sup>, José C. Quadrado<sup>1</sup>, Sónia Ferreira Pinto<sup>2</sup>, Duarte de Mesquita e Sousa<sup>2</sup>

<sup>1</sup> Instituto Superior de Engenharia de Lisboa, R. Conselheiro Emídio Navarro, 1959-007 Lisboa, Portugal

rluis@deea.isel.pt, jcquadrado@isel.pt

<sup>2</sup> Instituto Superior Técnico, Instituto Superior Técnico, INESC-id, DEEC, AC Energia Av. Rovisco Pais, 1049-001 Lisboa, Portugal

Fernando.alves@tecnico.ulisboa.pt, duarte.sousa@tecnico.ulisboa.pt, soniafp@tecnico.ulisboa.pt

**Abstract.** This paper presents the modelling and the numerical simulation results of a bidirectional DC-DC converter using modular Marx power electronic switches to be applicable in high-voltage converters. To achieve ample voltage ratio between high-voltage and low-voltage sides, the proposed DC-DC converter uses also a power electronic circuit, in the low-voltage converter side, that changes the connection between three inductors, as a series or parallel connection, to aid the energy transfer to the inductors.

**Keywords:** Bidirectional DC-DC converter; modular Marx switches; series-parallel inductor circuit.

## 1 Introduction

The recent industrial applications request energy storage systems (ESS) based on lithium-ion batteries banks and/or ultracapacitors cells for long-term energy storage or short-term energy storage, respectively. Examples of these applications can be seen in uninterruptible power supplies, hybrid powered traction systems, renewable energy generation, mobile energy generation and integrated active filters.

The control of the charge and discharge modes of the ESS need a bidirectional power electronic interface between the storage banks and the loads or to higher voltage DC-bus systems generally used with three-phase inverters, active front-end rectifiers and other power converters topologies.

Due the low nominal voltage of this batteries and ultracapacitors cells, it is required a large voltage conversion ratio for bidirectional DC-DC converter. In case of ultracapacitors their wide variation voltage in charging and discharging operation make difficult to design a bidirectional DC-DC converter with high voltage ratio.

In the last decade several works has been done to design solutions for bidirectional DC-DC converters. A good review can be found in [1][2], where the main isolated and non-isolated bidirectional converter topologies are deployed.

In this paper, the proposed power electronic converter is a bidirectional non isolated half-bridge DC-DC converter based on buck-boost converter, [3]. To make the converter able to high-voltage applications, it uses a series-stacked semiconductors based on solid-state Marx generator concept, [4]. Using a Marx generator as a series switch, allows the use of low-voltage semiconductors and arrange the overall structure of the DC-DC converter with modular cells, which leads to compactness, low weight, low cost and portability of these power converters, [4].

The Fig. 1 presents the bidirectional DC-DC converter employing six modules of Marx cells and series-parallel inductor electronic circuit.

The modular Marx power electronic switches,  $SM_1$  and  $SM_2$ , each one, uses three modular Marx cells. The HV side voltage, in steady-state operation, will be the sum of the capacitors voltage,  $v_{Ck}$ , for each three cells of  $SM_1$  or  $SM_2$ .

To right operation of the bidirectional DC-DC converter, the DC voltage capacitor balancing should be taking account, using some strategies to equalize the  $v_{Ck}$ , which also depends of modular Marx cells quantity used, [5][6].

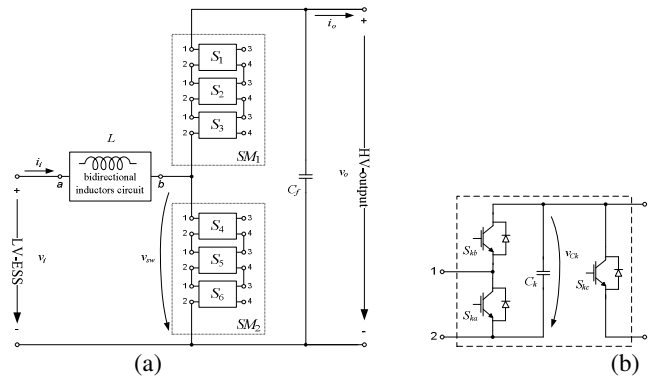


**Fig. 1.** Bidirectional DC-DC converter using Marx power switches and series-parallel inductor circuit: (a) the proposed bidirectional DC-DC power electronic converter; (b) the modular Marx power electronic cell.

## 2 Contribution to Collective Awareness Systems

This paper proposes a bidirectional DC-DC power converter using modular Marx switches to achieve high voltage ratios. The bidirectional DC-DC power electronic converters together with the energy storage systems have significant importance to overcome the power availability issues of renewable energy sources. Also other applications for bidirectional DC-DC converters, as electric traction systems, have a

remarkable position in sustainable growth. Due the application of modular cells in this DC-DC converter and also the proposed solution to achieve high voltage ratios, this work also allows the development of new technologies, which should be accounted in sustainability-aware decisions for collective awareness systems.

### 3 Series-parallel Inductor Electronic Circuit

The design of the inductor  $L$  assumes considerable importance, since it is responsible for the power transfer, in both directions, between the low-voltage (LV) to high-voltage (HV) sides. The sizing of the inductor  $L$  determines also the LV side current ripple and the switching frequency of the DC-DC converter.

In this work, the inductor  $L$  can switch from a parallel to a series arrangement through the use of bidirectional semiconductor circuit that changes between connections to obtain high voltage ratios from LV to HV sides.

Fig.2(a) presents the series-parallel inductor electronic circuit (SPIEC) with three non-coupled inductors,  $L_1, L_2, L_3$ , the semiconductors for parallel inductor connection,  $S_{P1}, S_{P2}, S_{P3}, S_{P4}$  and the semiconductors for series inductor connection,  $S_{S1}, S_{S2}$ . The terminals  $a$  and  $b$  represent the input and output of this electronic circuit.

The Fig.2(b) presents one cell of SPIEC, that can be used to extend this concept to higher number of non-coupled inductor connections, where  $k = \{1, 2, \dots, m + 1\}$  and  $m$  the total number of SPIEC cells.

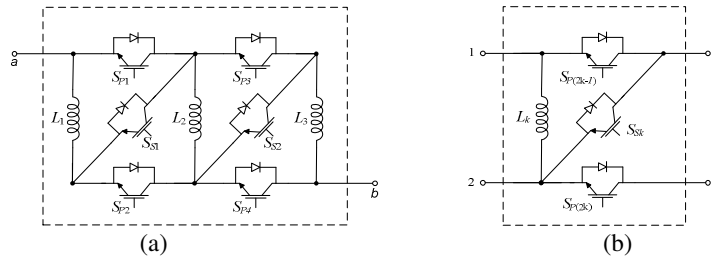


**Fig. 2.** The series-parallel inductor electronic circuit: (a) example of SPIEC with three inductors; (b) the SPIEC module cell.

Considering the SPIEC operating in the bidirectional DC-DC converter the voltage ratio from HV to LV sides can be deduced taking account the duty cycle,  $\delta$ , of switching period,  $T$ , of modular Marx switches,  $SM_1, SM_2$  and the number of SPIEC cells,  $m$ .

The Fig. 3 presents an example of two SPIEC modular cells (three non-coupled inductors).

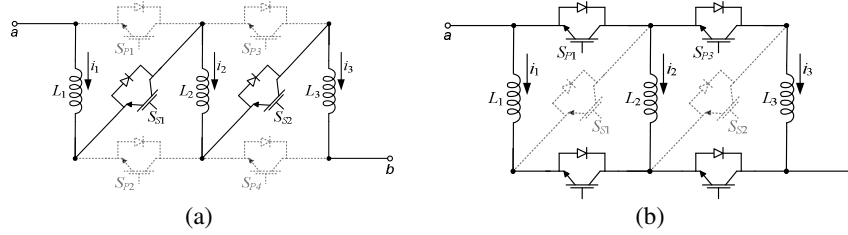


**Fig. 3.** The series-parallel inductor electronic circuit: (a) parallel mode operation; (b) series mode operation.

Starting from parallel inductors connection, represented in Fig.3(a), the  $S_{S1}$  and  $S_{S2}$  semiconductors are synchronised with  $S_1$  (which is turned Off) and  $S_{P1}$ ,  $S_{P2}$ ,  $S_{P3}$  and  $S_{P4}$  are tuned with  $S_2$  (which is On) during time  $\delta T$ . Being  $v_{L1}$ ,  $v_{L2}$ ,  $v_{L3}$  the voltage across the inductors  $L_1$ ,  $L_2$  and  $L_3$  respectively and  $v_i$  the voltage of LV source, then  $v_{L1} = v_{L2} = v_{L3} = v_i$ .

For series inductors connection, represented in Fig.3(b), the  $S_{S1}$  and  $S_{S2}$  semiconductors are synchronised with  $S_1$  (which is turned On) and  $S_{P1}$ ,  $S_{P2}$ ,  $S_{P3}$ ,  $S_{P4}$  tuned with  $S_2$  (which is Off) during time  $(1 - \delta) T$ . If  $v_o$  represents the voltage of HV side of DC-DC power converter, then  $v_{L1} + v_{L2} + v_{L3} = v_i - v_o$ . Considering equal inductors, where  $v_L$  is the voltage across each inductor, the previous equation can be rewritten as (1).

$$v_L = \frac{v_i - v_o}{3} \tag{1}$$

Considering the SPIEC steady-state operation with inductors current at continuous mode, the integral of the voltage across each inductor is zero over a cycle of switching  $T$ , which leads to (2).

$$\delta v_i + (1 - \delta) \frac{v_i - v_o}{3} = 0 \tag{2}$$

From (2) the voltage ratio of DC-DC converter can be found as (3).

$$\frac{v_o}{v_i} = \frac{2\delta + 1}{1 - \delta} \tag{3}$$

Generalizing (3) for different number of non-coupled inductors,  $n$ , the voltage ratio of DC-DC converter becomes (4).

$$\frac{v_o}{v_i} = \frac{(n - 1)\delta + 1}{1 - \delta} \tag{4}$$

Fig.4 presents the voltage ratio of (4) for two, three and four non-coupled inductors considering duty cycles varying from 0.4 to 0.9 and ideal circuit parameters.

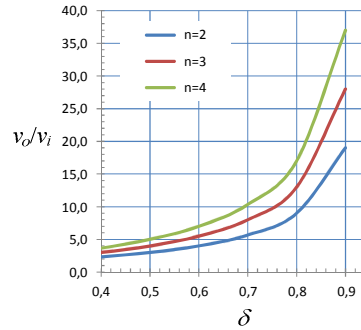


Fig. 4. Voltage ratios with different number of inductors and duty cycle values.

From Fig.4 and considering acceptable values for duty cycle between 0.7 and 0.8 the voltage ratio of the DC-DC converter can be change from 6 to 17 times dependent of the non-coupled inductors number used in SPIEC.

## 5 Switching Control Loops

The switching control loops necessary to the bidirectional DC-DC converter operation are depicted in Fig. 5.

To control the output voltage from HV side, is used a proportional-integral controller (PI), that based on voltage error,  $(v_{oref} - v_o)$ , produces an input current reference,  $i_{iref}$ , to LV side in inner current control loop. On other hand, this inner control loop uses a current hysteresis controller that generates the switching state,  $\gamma$ , associated with  $SM_1$  and  $SM_2$ .

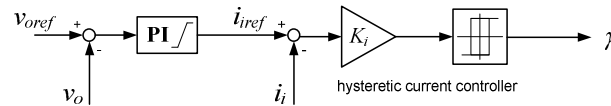


Fig. 5. Switching control loops of bidirectional DC-DC converter.

The PI controller has an internal limiter, to avoid overcurrents in the inner control loop, with an anti-windup system to prevent the accumulation of integral error when that limiter is active. The tuning of PI controller can be made using the linear control theory or the well know Ziegler-Nichols method, [7], considering a linearized closed loop transfer function of current controller  $i_i/i_{iref} \approx 1/(sT_d + 1)$ , where  $T_d$  is the average current delay related to the switching frequency of bidirectional DC-DC converter, [8].

From Fig.1, analysing the turn-on and turn-off signals associated with variable  $\gamma$  from the pulsed voltage across  $SM_2$ ,  $v_{sw}$ , follows, (5).

$$v_{sw} = \begin{cases} v_o & \text{if } SM_1 \text{ is ON ; } (\gamma=1) \\ 0 & \text{if } SM_2 \text{ is ON ; } (\gamma=0) \end{cases} \quad (5)$$

The state-space model that describes the dynamic of input current,  $i_i$ , considering that ( $v_{sw} = \gamma v_o$ ) is (6).

$$L \frac{di_i}{dt} = u_i - u_{sw} = u_i - \gamma u_o \quad (6)$$

To control the SPIEC input current,  $i_i$ , its current error,  $e_i$ , should be zero. However, since the bidirectional DC-DC converter is operated at finite frequency, the current error is maintained with a small ripple, (7).

$$e_i = i_{iref} - i_i \approx 0 < \mathcal{E} \quad (7)$$

The hysteretic current controller, from Fig.5, uses a hysteresis band of width  $2\mathcal{E}$  to maintain the input current error between:  $-\mathcal{E} < e_i < +\mathcal{E}$ . The command strategy that decides  $\gamma$  is given by (8).

$$\begin{cases} e_i > +\mathcal{E} \Rightarrow i_{iref} > i_i \Rightarrow i_i \uparrow \Rightarrow \frac{di_i}{dt} > 0 \Rightarrow v_{sw} = 0 \Rightarrow \gamma = 0 \\ e_i < -\mathcal{E} \Rightarrow i_{iref} < i_i \Rightarrow i_i \downarrow \Rightarrow \frac{di_i}{dt} < 0 \Rightarrow v_{sw} = v_o \Rightarrow \gamma = 1 \end{cases} \quad (8)$$

The hysteretic current controller uses also a gain,  $K_i$ , to adjust the variable switching frequency,  $f_s$ , within the semiconductors operating limits, [8], (9).

$$f_s = \frac{u_i(u_o - u_i)}{2\mathcal{E}K_i L u_o} \quad (9)$$

## 6 Numerical Simulation Results

The numerical simulation results of bidirectional DC-DC converter were performed with Matlab<sup>®</sup>/Simulink<sup>®</sup> and uses the SimPowerSystems<sup>™</sup> toolbox to include the losses of semiconductors, inductors and capacitors.

The main circuit parameters are:  $v_i = 1.5\text{kV}$ ;  $v_{oref} = 15\text{kV}$ ;  $L_k = 1\text{mH}$ ;  $C_f = 10\mu\text{F}$ ;  $2\mathcal{E} = 10\text{A}$ . To simulate different load conditions, an output current source on HV side was considered, where the  $i_o$  values and simulation time,  $t$ , intervals are:  $i_o = 0\text{A}$  (no load),  $t \in [0; 0.02]$ ;  $i_o = 15\text{A}$  (discharging LV side),

$t \in [0.02; 0.08]$ ;  $i_o = 15A$  (charging LV side),  $t \in [0.08; 0.14]$ . Since a voltage ratio of 10 is needed, for a  $\delta \cong 0.8$  three non-coupled inductors are used (Fig.4).

Fig. 6 presents the results of bidirectional DC-DC converter with three non-coupled inductors in SPIEC and Fig.7 presents a zoom view in load transient at 0.08s.

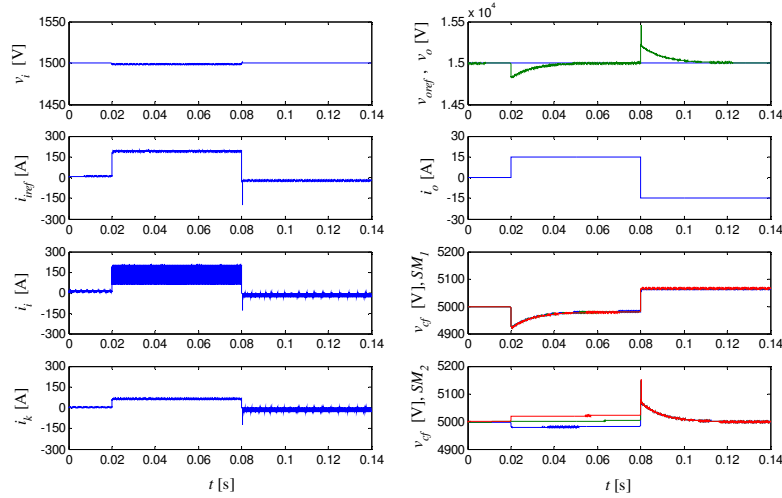


Fig. 6. Simulation results of bidirectional DC-DC converter.

From Fig.6, the DC-DC converter keeps a gain of 10 in voltage ratio. Due the load transients, the output voltage and the balance of voltage capacitors in Marx cells are tracked with variations about 3%.

In Fig.7 it is shown that the inductor currents have high ripple (210%), while the LV side current displays a ripple of 94% related with their reference values.

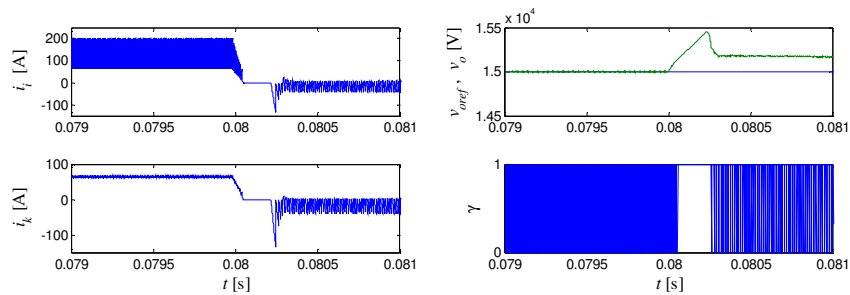


Fig. 7. The load transient in bidirectional DC-DC converter.



## 7 Conclusions

This paper presents the application of modular Marx cells in a bidirectional DC-DC power converter for HV applications. The high voltage ratio depends of non-coupled inductors number used in SPIEC and the duty cycle.

The balance of the Marx capacitor of the need stack cells remaining under 3%, while the output voltage has a ripple below 0.1%.

The developed simulation model is valuable as a proof of concept and to mitigate some drawbacks as the high ripple current in LV side.

## Acknowledgments

This work was supported by Portuguese national funds through FCT - Fundação para a Ciência e a Tecnologia, under project PEst-OE/EEI/LA0021/2013.

## References

1. S. Kumar and H. P. Ikkurti, "Design and control of novel power electronics interface for battery-ultracapacitor hybrid energy storage system," *Int. Conf. Sustain. Energy Intell. Syst.*, no. SEISCON, pp. 236–241, 2011.
2. R. M. Schupbach and J. C. Balda, "Comparing DC-DC converters for power management in hybrid electric vehicles," in *Electric Machines and Drives IEEE International Conference*, 2003.
3. H. R. Karshenas, H. Daneshpajoo, A. Safaee, P. Jain, and A. Bakhshai, "Bidirectional DC-DC Converters for Energy Storage Systems," in *Energy Storage in the Emerging Era of Smart Grids*, R. Carbone, Ed. InTech, 2011, p. 18.
4. L. Redondo and J. Fernando Silva, "Solid State Pulsed Power Electronics," in *Power Electronics Handbook*, Third Edit., Elsevier Inc., 2011, pp. 669–707.
5. L. Encarnação, J. F. Silva, S. F. Pinto, and L. M. Redondo, "Grid Integration of Offshore Wind Farms Using Modular Marx Multilevel Converters," in *Doctoral Conference on Computing, Electrical and Industrial Systems, DoCEIS'12*, 2012, pp. 311–320.
6. L. Encarnação, J. F. Silva, S. F. Pinto, and L. M. Redondo, "A New Modular Marx Derived Multilevel Converter," in *2nd Doctoral Conf. on Computing Electrical and Industrial Systems – DoCEIS Costa da Caparica, Portugal (2011)*, 2011, pp. 573–580.
7. K. Ogata, *Modern Control Engineering*, 5th Ed. Prentice Hall, 2010.
8. J. Fernando Silva, *Sistemas de Conversão Comutada: Semicondutores e Conversores Comutados de Potência*. Lisboa: AC Energia/DEEC/IST, 2012. (in portuguese)